J|A|C|S
ARTICLES
Published on Web 04/10/2003

Polyunsaturated Dicarboxylate Tethers Connecting Dimolybdenum Redox and Chromophoric Centers: Absorption Spectra and Electronic Structures

F. Albert Cotton,*,† James P. Donahue,† Carlos A. Murillo,*,† and Lisa M. Pérez‡

Contribution from the Department of Chemistry, Laboratory for Molecular Structure and Bonding, P.O. Box 30012, Texas A&M University, College Station, Texas 77842-3012 and Department of Chemistry, Laboratory for Molecular Simulation, P.O. Box 30012, Texas A&M University, College Station, Texas 77842-3012

Received January 27, 2003; E-mail: cotton@tamu.edu; murillo@tamu.edu

Abstract: The absorption spectra of a series of compounds of the type $[Mo_2(DAniF)_3](O_2CXCO_2)[Mo_2(DAniF)_3]$ (DAniF = *N,N′*-di-*p*-anisylformamidinate) have been measured and revealed a strong dependence of the electronic transitions and, therefore, the colors upon the chemical nature of the dicarboxylate linker. The more intense colors and lower energy absorptions are observed with those compounds having unsaturated dicarboxylate linkers. Static and time-dependent DFT calculations were undertaken to identify the electronic excitations responsible for the observed colors. For those compounds with chemically unsaturated and fully conjugated dicarboxylate linkers (oxalate, **6**; fumarate, **8**; acetylene dicarboxylate, **9**; *cis*,*cis*-muconate, **11**; *trans*,*trans*-muconate, **12**; tamuate, **13**; texate, **14**; terephthalate, **15**), the lowest energy absorptions are Mo_2^{4+} $\delta \rightarrow$ dicarboxylate π^* metal-to-ligand charge transfer transitions. Those compounds with chemically saturated linkers (succinate, **20**) have $\delta \rightarrow \delta^*$ transitions as their lowest energy absorptions with essentially independent and noninteracting Mo_2^{4+} chromophores.

Introduction

Interaction of light and matter is a subject of great importance in many areas ranging from photoactive devices to life processes.[1] For example, a topic of fundamental interest is the light harvesting photosynthetic process whereby light energy is converted into chemical energy. This process is mediated by carotenoids, which actively participate by absorbing energy in a fashion complementary to the role of chlorophylls.[2] Carotenoids also function as photoprotective agents by quenching excited triplet states of chlorophylls, a process in which the conversion of violaxanthin to zeaxanthin plays an important role.[3] Yet another important system is the visual cycle, where a cis to trans isomerization of rhodopsin is triggered by light.[4] In this process, an important precursor is retinoic acid, which is formed by the oxidative cleavage of β-carotene (Chart 1).

Carotenoids have been the subject of extensive studies because of the role they play in such vital biological functions as respiration, health and immunology, and antioxidant chemistry at the cellular level.[5] For instance, it has been proposed that carotenoids function as antioxidants by quenching singlet oxygen, peroxyl radicals, and other radicals formed during lipid oxidation, such as the lipid radicals formed by hydrogen abstraction from allylic CH_2 groups of some polyunsaturated

Chart 1. Examples of Carotenes or Carotene Derivatives

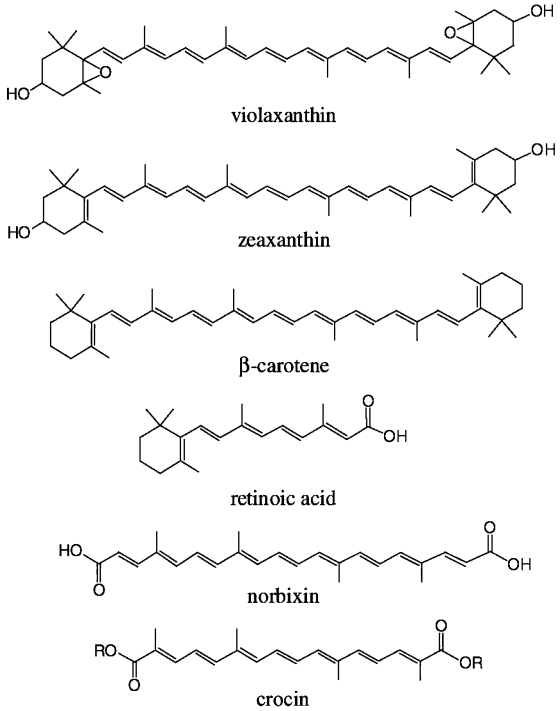

† Laboratory for Molecular Structure and Bonding, Texas A&M University.

‡ Laboratory for Molecular Simulation, Texas A&M University.

(1) For example, see: (a) Comorosan, S.; Jieanu, V.; Morlova, I.; Paslaru, L.; Rozoveanu, P.; Toroiman, E.; Vasilco, R. *Physiol. Chem. Phys. Med. NMR* **1988**, *20*, 319. (b) Comorosan, S. *J. Biol. Phys.* **1990**, *17*, 151. (c) Brixner, T.; Damrauer, N. H.; Gerber, G. *Adv. At., Mol., Opt. Phys.* **2001**, *46*, 1.
(2) Wang, Y.; Hu, X. *J. Am. Chem. Soc.* **2002**, *124*, 8445.
(3) (a) Ruban, A. V.; Phillip, D.; Young, A. J.; Horton, P. *Biochemistry* **1997**, *36*, 7855. (b) Frank, H. A.; Bautista, J. A.; Josue, J. S.; Young, A. J. *Biochemistry* **2000**, *39*, 2831.
(4) Rando, R. R. *Chem. Rev.* **2001**, *101*, 1881.

10.1021/ja0343555 CCC: $25.00

Scheme 1. Generic Structure of a Dicarboxylate Linked Pair $[Mo_2(DAniF)_3](O_2CXCO_2)[Mo_2(DAniF)_3]$, Including the Structure of the *N,N′*-Di-*p*-anisylformamidinate (DAniF) Ligand

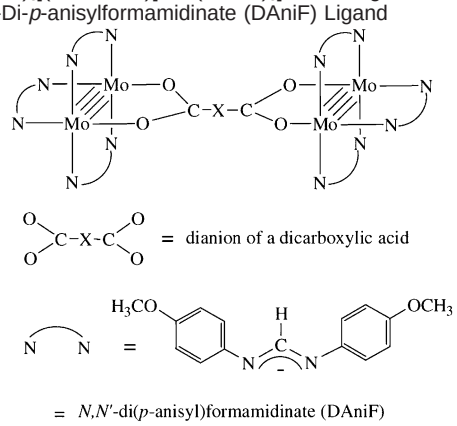

fatty acids. Physical quenching is believed to occur by energy transfer from the excited oxygen species to the carotenoid, yielding a triplet carotenoid.[6] Because of the extensive π conjugation, the energy of the excited carotenoid is likely dissipated through vibrational interactions.

The interaction of light with transition metal complexes is also a vast field of study. Here, electronic transitions between d orbitals and ligand-to-metal or metal-to-ligand charge transfers are responsible for the colors of these complexes. The study of electronic transitions provides a window upon the electron distribution and relative energies of the various orbitals in a given crystal field environment. These studies may be extended to systems with more than one metal center. Compounds that have dimetal units with metal−metal bonding represent an area that has been the subject of numerous spectroscopic studies and theoretical analyses.[7] For instance, the electronic absorption spectra of $Mo_2(O_2CR)_4$ complexes have been examined in great detail in an effort to establish unequivocally the $\sigma^2\pi^4\delta^2$ electronic configuration for the quadruple bond and identify the $\delta \rightarrow \delta^*$ transition, which generally is the HOMO → LUMO excitation when R is a simple alkyl substituent such as CH_3.[8]

In prior work,[9] we have described the syntheses, structures, and electrochemistry of an extensive set of dicarboxylate-linked compounds of the type $[Mo_2(DAniF)_3](O_2CXCO_2)[Mo_2(DAniF)_3]$

Chart 2. List of $Mo_2(DAniF)_3(O_2CX)$ and $[Mo_2(DAniF)_3](\mu\text{-}O_2CXCO_2)[Mo_2(DAniF)_3]$ Compounds as Identified by Their Mono- or Dicarboxylate Ligands

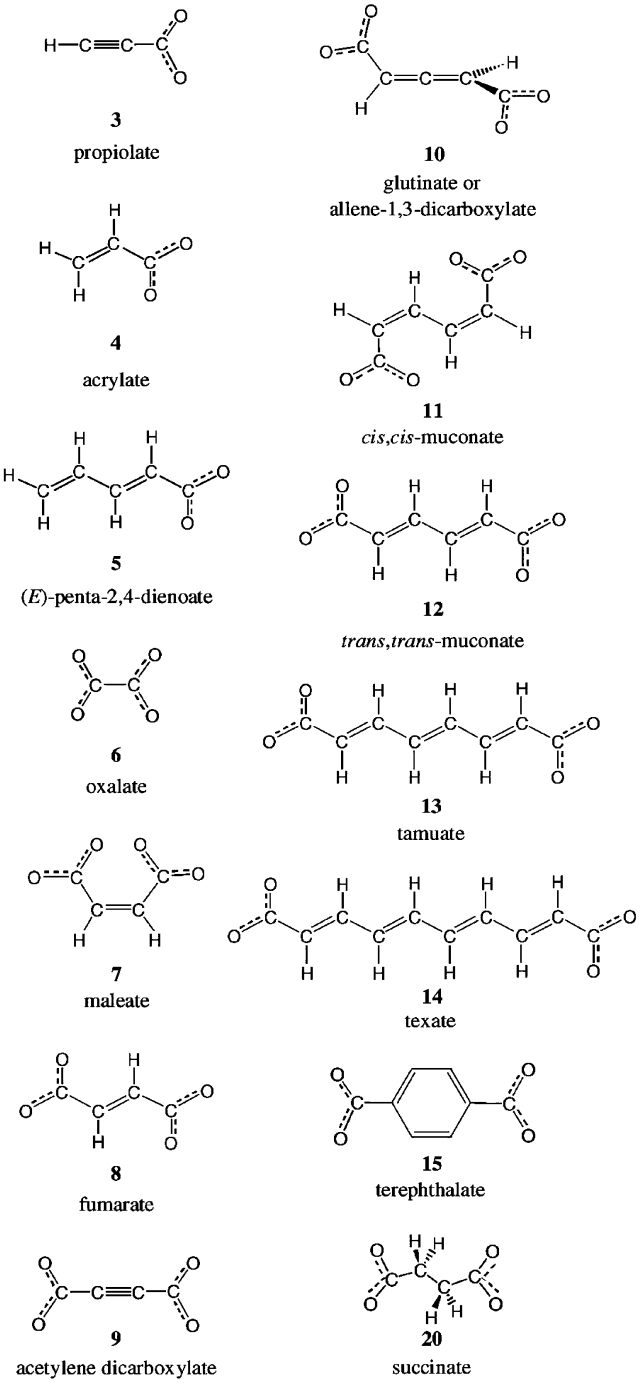

(DAniF = *N,N′*-di-*p*-anisylformamidinate), the general structure of which is set forth in Scheme 1. A selection of such compounds is presented in Chart 2, where the molecules are identified by their dicarboxylate linkers and the numbering system used in the preceding report[9b] is retained here. We have observed that the colors of such complexes are highly dependent upon the nature of the dicarboxylate ligand. For instance, the set of compounds $Mo_2(DAniF)_3(O_2CCH_nCH_nCO_2)Mo_2(DAniF)_3$ (n = 0, 1, 2), in which two quadruply bonded Mo_2 units are linked by a dicarboxylate dianion, reveals dramatic color changes in moving from the molecule with the fully saturated dicarboxylate linker (bright yellow) to that with an olefinic bond

(5) For example, see: Nishino, H. In *Functional Foods for Disease Prevention I*; Shibamoto, T., Terao, J., Osawa, T., Eds.; ACS Symposium Series 701; American Chemical Society: Washington, DC, 1998; p 59 and references therein.

(6) (a) Mortensen, A.; Skibsted, L. H. *J. Agric. Food Chem.* **1997**, *45*, 2970. (b) Kappus, H. In *Free Radicals and Food Additives*, Arouma, O. I., Halliwell, B., Eds.; Taylor and Francis: London, 1991; p 59. (c) Garavelli, M.; Bernardi, F.; Olivucci, M.; Robb, M. A. *J. Am. Chem. Soc.* **1998**, *120*, 10210. (d) Mortensen, A.; Everett, S. A.; Skibstead, L. H. In *Phytochemicals and Phytopharmaceuticals*; Shahidi, F., Ho, C.-T., Eds; AOCS Press: Champaign, IL 2000; p 185.

(7) (a) Cotton, F. A.; Walton, R. A. *Multiple Bonds Between Metal Atoms*; Clarendon: Oxford, 1993. (b) Hopkins, M. D.; Gray, H. B.; Miskowski, V. M. *Polyhedron* **1987**, *6*, 705. (c) Miskowski, V. M.; Hopkins, M. D.; Winkler, J. R.; Gray, H. B. In *Inorganic Electronic Structure and Spectroscopy*; Solomon, E. I., Lever, A. B. P., Eds.; Wiley: New York, 1999; Vol. 2, pp 343−402. (d) Beers, W. W.; McCarley, R. E.; Martin, D. S.; Miskowski, V. M.; Gray, H. B.; Hopkins, M. D. *Coord. Chem. Rev.* **1999**, *187*, 103. (e) Cotton, F. A.; Nocera, D. G. *Acc. Chem. Res.* **2000**, *33*, 483.

(8) (a) Cotton, F. A.; Martin, D. S.; Fanwick, P. E.; Peters, T. J.; Webb, T. R. *J. Am. Chem. Soc.* **1976**, *98*, 4681. (b) Martin, D. S.; Newman, R. A.; Fanwick, P. E. *Inorg. Chem.* **1979**, *18*, 2511. (c) Cotton, F. A.; Martin, D. S.; Webb, T. R.; Peters, T. J. *Inorg. Chem.* **1976**, *15*, 1199. (d) Martin, D. S.; Huang, H.-W. *Inorg. Chem.* **1990**, *29*, 3674. (e) Cotton, F. A.; Zhong, B. *J. Am. Chem. Soc.* **1990**, *112*, 2256. (f) Chisholm, M. H.; Huffman, J. C.; Iyer, S. S.; Lynn, M. A. *Inorg. Chim. Acta* **1996**, *243*, 283.

(9) (a) Cotton, F. A.; Donahue, J. P.; Lin, C.; Murillo, C. A. *Inorg. Chem.* **2001**, *40*, 1234. (b) Cotton, F. A.; Donahue, J. P.; Murillo, C. A. *J. Am. Chem. Soc.* **2003**, *125*, 5436.

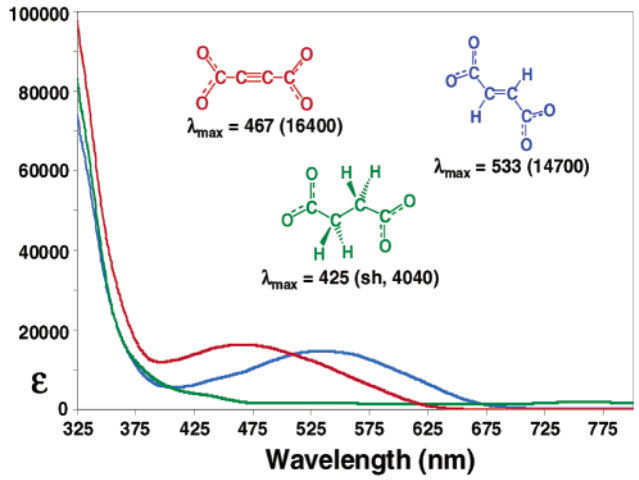

Figure 1. UV−vis spectra illustrating the effect of the degree of saturation in the series of molecules $[Mo_2(DAniF)_3](O_2CCH_nCH_nCO_2)[Mo_2DAniF)_3]$, ($n$ = 0, 1, 2). Compounds are identified by the dicarboxylate linker.

(deep violet) to that with an acetylenic bond (bright red) (Figure 1). In view of what is already known about $Mo_2(O_2CR)_4$ and $Mo_2(RNC(H)NCR)_4$[10] compounds, we were inclined to attribute these effects to some form of metal-to-ligand charge transfer involving the δ orbitals of the Mo_2^{4+} units. We have therefore measured the absorption spectra of all the new compounds whose syntheses are described in our earlier reports[9] and employed both static and time-dependent DFT calculations to ascertain their electronic structures and to identify the particular transitions that are responsible for the lowest energy absorption in each case. For comparison to the linked molecules, the electronic spectra of unlinked paddlewheel complexes of the type $Mo_2(DAniF)_3(O_2CX)$ (X = C≡CH, CH=CH_2, CH=CH−CH=CH_2) have also been examined. Computational studies by Bursten and Chisholm upon the oxalate and perfluoroterephthalate-bridged molecules $(Bu^tCO_2)_3M_2(\mu\text{-}O_2CCO_2)M_2(O_2CBu^t)_3$ and $(Bu^tCO_2)_3M_2(\mu\text{-}O_2CC_6F_4CO_2)M_2(O_2CBu^t)_3$ (M = Mo, W) appeared recently and reveal the principal feature in the electronic spectra to be an M_2 $\delta \rightarrow$ oxalate or perfluoroterephthalate π^* metal-to-ligand charge transfer.[11] Our results are consistent with the work of Bursten and Chisholm but extend the study to a wider variety of dicarboxylate linked compounds and provide experimental data to compare against theoretically derived values.

We observe that some of the highly unsaturated dicarboxylate linkers we have used are small-molecule analogues of certain carotenoids, such as norbixin and crocin (Chart 1), which are themselves polyolefinic dicarboxylic acids or their ester derivatives. We further note that carotenoid-like molecules have been prepared and studied as components of possible molecule-scale devices, such as transmembrane molecular wires[12] and covalent connectors in photoactive donor−acceptor systems.[13] In view of these broader research interests, we recognize the value of developing an improved understanding of how such polyolefinic connecting ligands can both mediate electronic communication between redox centers and modulate the electronic structures of transition metal chromophores. Conceivably, a multiply bonded M_2 chromophore bound by a polyolefinic carboxylic acid might usefully serve as a spectroscopic probe of the photophysics of carotenoid molecules.

Experimental Section

Physical Methods. Absorption spectra were measured at room temperature under N_2 using a Shimadzu UV-1601PC spectrophotometer. All spectra were recorded in distilled CH_2Cl_2 using quartz cuvettes with a 1.0 cm path length.

Computational Details. All calculations were performed with the Gaussian 98 (G98) suite of programs[14] using a double-ζ basis set (D95) on the C, N, O, and H atoms.[15] A small (1s2s3s2p3p3d) effective core potential (ECP) was used for the Mo atoms with a double-ζ quality basis set.[16] To investigate the electronic structures of compounds **3**−**15** and **20**, single point energy calculations[17] were performed using density functional theory (DFT)[18] with the Becke three parameter hybrid exchange functional[19] and the Lee−Yang−Parr correlation functional (B3LYP).[20] For feasibility purposes, the calculations were simplified by replacing each *p*-anisyl substituent with a hydrogen atom. To gain insight into the electronic transition responsible for the observed UV−vis spectra of **3**−**15** and **20**, time-dependent density functional theory[21] (TDDFT) calculations were performed on an SGI Power Challenge, Origin 2000, and Origin 3800 computer at the Texas A&M University Supercomputing facility and on an SGI Power Challenge in the Department of Chemistry, Texas A&M University.

Results and Discussion

In the absorption spectra of the series of five compounds $[Mo_2(DAniF)_3](O_2C(CH{=}CH)_nCO_2)[Mo_2(DAniF)_3]$ (n = 0−4) (Figure 2), a very important feature is the lowest energy transition. As the linker is lengthened with carbon−carbon double bonds, this transition shifts to lower energy and higher intensity. Upon the addition of the first carbon−carbon double bond, the effect is quite pronounced, but the absorption maxima appear to approach an asymptotic limit as further olefinic bonds are added. By extrapolation, a prediction can be made that the member of this series with n = 5 should have a maximum at ~586 nm (17 100 cm^{-1}) with a molar extinction coefficient of ~20 000. It should be noted that the high ϵ values are not consistent with these absorptions being $\delta \rightarrow \delta^*$ transitions, which, though not symmetry forbidden, occur with relatively

(10) Cotton, F,. A.; Feng, X.; Matusz, M. *Inorg. Chem.* **1989**, *28*, 594.
(11) (a) Bursten, B. E.; Chisholm, M. H.; Hadad, C. M.; Li, J.; Wilson, P. J. *Chem. Commun.* **2001**, 2382. (b) Bursten, B. E.; Chisholm, M. H.; Clark, R. J. H.; Firth, S.; Hadad, C. M.; MacIntosh, A. M.; Wilson, P. J.; Woodward, P. M.; Zaleski, J. M. *J. Am. Chem. Soc.* **2002**, *124*, 3050 (c) Bursten, B. E.; Chisholm, M. H.; Clark, R. J. H.; Firth, S.; Hadad, C. M.; Wilson, P. J.; Woodward, P. M.; Zaleski, J. M. *J. Am. Chem. Soc.* **2002**, *124*, 12244.
(12) Arrhenius, T. S.; Blanchard-Desce, M.; Dvolaitzky, M.; Lehn, J.-M.; Malthete, J. *Proc. Natl. Acad. Sci. U.S.A.* **1986**, *83*, 5355.
(13) Slama-Schwok, A.; Blanchard-Desce, M.; Lehn, J.-M. *J. Phys. Chem.* **1990**, *94*, 3894.
(14) Frisch, M. J.; Trucks, G. W.; Schlegel, H. B.; Scuseria, G. E.; Robb, M. A.; Cheeseman, J. R.; Zakrzewski, V. G.; Montgomery, J. A.; Stratmann, R. E.; Burant, J. C.; Dapprich, S.; Millam, J. M.; Daniels, A. D.; Kudin, K. N.; Strain, M. C.; Farkas, O.; Tomasi, J.; Barone, V.; Cossi, M.; Cammi, R.; Mennucci, B.; Pomelli, C.; Adamo, C.; Clifford, S.; Ochterski, J.; Petersson, G. A.; Ayala, P. Y.; Cui, Q.; Morokuma, K.; Malick, D. K.; Rabuck, A. D.; Raghavachari, K.; Foresman, J. B.; Cioslowski, J.; Ortiz, J. V.; Stefanov, B. B.; Liu, G.; Liashenko, A.; Piskorz, P.; Komaromi, I.; Gomperts, R.; Martin, R. L.; Fox, D. J.; Keith, T.; Al-Laham, M. A.; Peng, C. Y.; Nanayakkara, A.; Gonzalez, C.; Challacombe, M.; Gill, P. M. W.; Johnson, B. G.; Chen, W.; Wong, M. W.; Andres, J. L.; Head-Gordon, M.; Replogle, E. S.; Pople, J. A. *Gaussian 98*, revisions A.6, A.7, and A.9; Gaussian, Inc.: Pittsburgh, PA, 1998.
(15) Dunning, T. H.; Hay, P. J. *Methods of Electronic Structure Theory*; Schaefer, H. F., III, Ed.; Plenum Press: New York, 1977; Vol. 3.
(16) Hay, P. J.; Wadt, W. R. *J. Chem. Phys.* **1985**, *82*, 299.
(17) The convergence criterion for the SCF was increased from the default value of 10^{-4} to 10^{-8}.
(18) Parr, R. G.; Yang, W. *Density-Functional Theory of Atoms and Molecules*; Oxford University Press: Oxford, 1989.
(19) (a) Becke, A. D. *Phys. Rev. A.* **1998**, *38*, 3098. (b) Becke, A. D. *J. Chem. Phys.* **1993**, *98*, 1372. (c) Becke, A. D. *J. Chem. Phys.* **1993**, *98*, 5648.
(20) Lee, C. T.; Yang, W. T.; Parr, R. G. *Phys. Rev. B* **1998**, *37*, 785.
(21) Casida, M. E.; Jaorski, C.; Casida, K. C.; Salahub, D. R. *J. Chem. Phys.* **1998**, *108*, 4439.

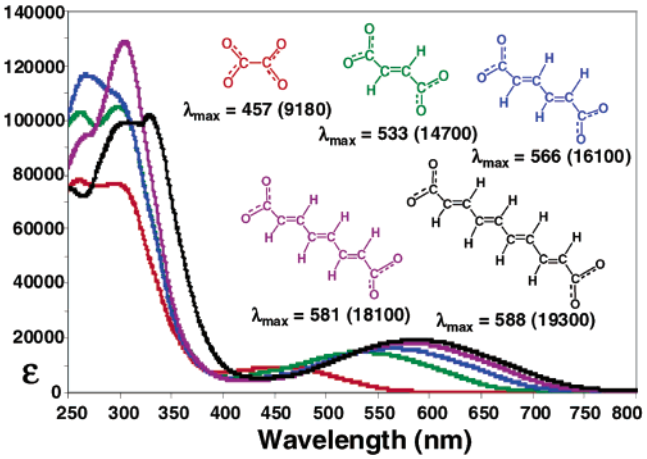

Figure 2. UV−vis spectra of the series $[Mo_2(DAniF)_3](O_2C(CH{=}CH)_n\text{-}CO_2)[Mo_2DAniF)_3]$ ($n = 0-4$). Compounds are identified by the dicarboxylate linker.

modest molar extinction coefficients of ~1000 because of low overlap of the d δ orbitals on the two metal atoms. Actually, the integrated intensities of the bands increase even more rapidly than the peak ϵ values, but again an asymptotic limit seems to be approached at about $n = 5$.

A comparison of the unbridged compounds **4** and **5** with their bridged counterparts **8** and **12** (Figure 3a) makes it clear that the latter pair constitute a whole which is not merely the sum of its parts. The lowest energy transition for the latter pair is shifted fairly dramatically to a longer wavelength and higher intensity. This shows that the transitions responsible for these absorptions involve molecular orbitals composed of *both* Mo_2^{4+} units as well as the dicarboxylate linker. A further insight is found in the comparison between **4** and the allene-1,3-dicarboxylate bridged molecule, **10** (Figure 3b). Qualitatively, the spectra for **4** and **10** are the same, the latter only differing in having greater intensity. The orthogonality of the two π bonds in the allenyl system causes the molecule to behave essentially as though it has two independent, uncoupled chromophores and emphasizes that the shifts to lower energy require a linker that is *both* unsaturated *and* conjugated such that the two Mo_2^{4+} units may communicate electronically.

Small differences are observed between the isomeric pairs **7**/**8** (Figure 4a) and **11**/**12** (Figure 4b). Each trans isomer has the lower energy and higher intensity absorption. In this connection, it should be noted that the trans molecules **8** and **12** are longer than the cis isomers **7** and **11** by 1.5 Å and 1.2 Å, respectively, as determined from their crystal structures. As a first approximation, these molecules may be viewed as a form of the one-dimensional particle-in-a-box situation.[22] Since the trans isomers **8** and **12** are physically longer, the first wave harmonic one could draw in them is lower in energy than the cis isomers **7** and **11**. This heuristic argument leads to the expectation that the intrinsically lower energy of the trans isomers is a general phenomenon. In this context, our observation that the lowest energy UV−vis absorption maxima of dimethyl *cis*,*cis*- and *trans*,*trans*-muconate lie at 260 and 263 nm, respectively, is consistent with this idea.

(22) Other instances are available in the literature in which the construct of a particle in a one-dimensional box is employed as a model for the description of conjugated systems. For example, see: (a) Calzaferri, G. *Chimia* **1987**, *41*, 248. (b) Chernyak, V.; Volkov, S. N.; Mukamel, S. *J. Phys. Chem. A* **2001**, *105*, 1988. (c) Rogers, J. E.; Cooper, T. M.; Fleitz, P. A.; Glass, D. J.; McLeans, D. G. *J. Phys. Chem. A.* **2002**, *106*, 10108.

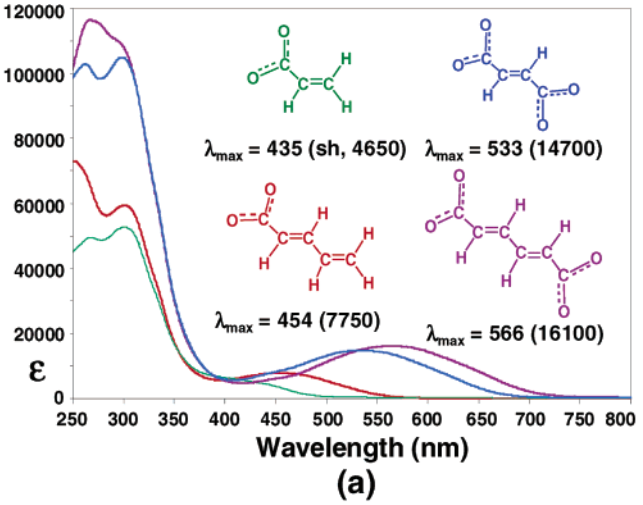

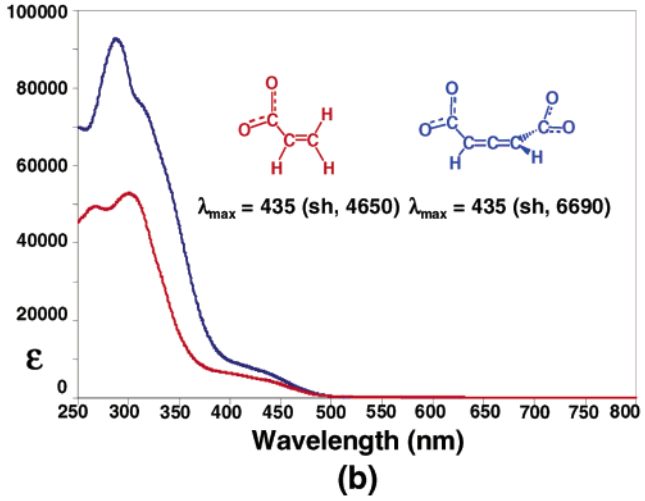

Figure 3. (a) UV−vis spectra of molecules **4** and **5** vs their linked counterparts **8** and **12**. (b) Comparison of the UV−vis spectra of **4** and the linked but nonconjugated molecule **10**. Compounds are identified by their carboxylate ligands.

The results of our time-dependent DFT calculations indicate that the dicarboxylate linked pairs $[Mo_2(DAniF)_3](O_2CXCO_2)[Mo_2(DAniF)_3]$ with unsaturated, conjugated dicarboxylate linkers have lowest energy absorptions that are of the same general nature. For these molecules, which include **6**, **8**, **9**, and **11**−**15**, the lowest energy absorption is a HOMO → LUMO metal-to-ligand charge transfer transition. This is clearly illustrated in Figure 5, which shows both the HOMO and LUMO for the series $[Mo_2(DAniF)_3](O_2C(CH{=}CH)_nCO_2)[Mo_2(DAniF)_3]$ ($n = 0-3$). The highest occupied molecular orbital in each case is centered on the Mo_2^{4+} units and is the Mo−Mo δ orbital. The phase of the δ orbitals of the Mo_2 units in the HOMO alternates with the number of olefinic bonds in the dicarboxylate tethers. As seen in Figure 5, molecule **6** has an antisymmetric combination with respect to a pseudo mirror plane between the Mo_2 units, while **8** is symmetric, **12** is antisymmetric, **13** is again symmetric, and **14** is antisymmetric. The lowest unoccupied molecular orbital is principally a dicarboxylate ligand-based π^* orbital. Clearly evident in the LUMOs illustrated in Figure 5 is the presence of nodes at each carbon−carbon double bond as well as between the oxygen and carbon atoms of the dicarboxylate chelate. As one might intuitively expect, the energy separation between the HOMO and the HOMO-1 diminishes

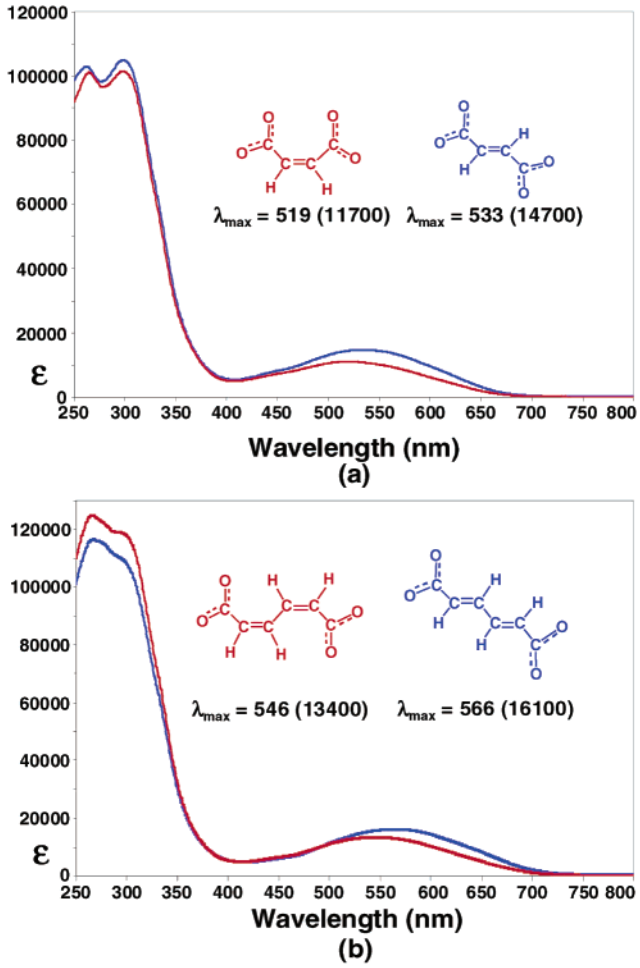

Figure 4. UV−vis spectra of $[Mo_2(DAniF)_3](O_2CXCO_2)[Mo_2DAniF)_3]$ compounds which are geometrical isomers: (a) **7** vs **8** and (b) **11** vs **12**. Compounds are identified by the dicarboxylate linker.

across the series $[Mo_2(DAniF)_3](O_2C(CH{=}CH)_nCO_2)[Mo_2(DAniF)_3]$ ($n = 0-4$).[23] As the length of the polyolefinic dicarboxylate is increased, other excitations begin to contribute to the lowest energy absorption, which accounts for the increased broadening of this band as n increases (Figure 2). Nevertheless, even when $n = 4$, the most important excitation is still the HOMO → LUMO transition.

In the unlinked molecules **3**−**5**, the lowest energy absorptions are also δ-to-π^* metal-to-ligand charge transfer transitions, but the π^* orbitals in these molecules are at appreciably higher energies relative to their bridged counterparts. The higher π^* energies in **3**−**5** stem from the lack of the second carboxylate group in the ligand. Compound **12**, for instance, has six p atomic orbitals with two nodes passing through the olefinic bonds of the dicarboxylate linker (Figure 5). This configuration has three π bonds. The unlinked molecule **5** has five p atomic orbitals with two nodes, one node lying between the two terminal carbon atoms of the pentadienoate ligand, which permits only two π bonds. Thus, compared to their unlinked analogues, linked molecules such as **8** or **12** will in general have a higher ratio of π bonding interactions to nodes and therefore will possess lower energy π^* orbitals.

(23) The energy separations between the HOMO and HOMO-1 are 6.7, 4.9, 4.0, 3.5, and 3.2 kcal/mol for molecules **6**, **8**, **12**, **13**, and **14**, respectively.

Table 1 lists the energies of these lowest energy transitions as determined experimentally and computationally, and Figure 6 graphically illustrates these data for the five-member series $[Mo_2(DAniF)_3](O_2C(CH{=}CH)_nCO_2)[Mo_2(DAniF)_3]$ ($n = 0-4$). Differences exist between these two sets of numbers, but qualitatively the trends are the same. For the series $[Mo_2(DAniF)_3](O_2C(CH{=}CH)_nCO_2)[Mo_2(DAniF)_3]$ ($n = 0-4$), the differences between the experimentally observed absorbances and the calculated transition energies increase as n increases. The transition energies calculated by DFT using partial geometry-optimized structures[24] define a fairly smooth curve (Figure 6) compared to the results obtained using the fixed structures from X-ray crystallography. For $n = 4$, the geometry optimized structure yields a result appreciably closer to the experimentally observed transition energy than does the crystal structure (Figure 6).[25]

The likely reason for the divergence between the DFT calculations and the experimentally observed transition energies is an overestimation by the DFT methodology of the extent of delocalization within the polyolefinic chain of the linker as the system increases in length.[26] It is known that, even in the limit of infinitely long conjugated polyolefins, the carbon−carbon bond distances are still alternately long (1.44 Å) and short (1.36 Å).[27] This effect can be considered as a form of Peierls distortion that, relative to the fully delocalized system, lowers the overall energy of the π orbitals that are occupied while raising the π^* orbitals that are unoccupied. By not accurately accounting for the alternating carbon−carbon bond lengths in the dicarboxylate linkers, the DFT calculations underestimate the energies of their π^* orbitals and produce $\delta \rightarrow \pi^*$ transition energies that fall below the observed values.

For the maleate bridged molecule, **7**, the composition of its HOMO and LUMO is belied by its relatively simple spectrum. As observed in our previous report,[9b] this molecule is distorted from planarity by the steric crowding between *p*-anisyl groups of the formamidinate ligands of opposing Mo_2^{4+} units. The off-axis twist of one Mo_2 unit with respect to the other actually occurs within the maleate linker itself between the carbon−carbon bond of the alkene unit and one of the carboxylate moieties. Our DFT calculations suggest that the effect of this distortion is to modify the nature of the LUMO by diminishing its π^* character and introducing some σ character between this dicarboxylate and one of the Mo_2 units. The HOMO is also of diminished δ character and now bears some contributions from the other atoms of the molecule. Thus, while the lowest energy absorption of **7** is still a HOMO → LUMO transition, the composition of these orbitals is appreciably different from those molecules with essentially planar core structures.

The remaining dicarboxylate linked pairs are molecules having a lowest energy absorption that is different in nature

(24) The dicarboxylic acid analogue of the dicarboxylate linkers in **6**, **8**, **12**, **13**, and **14** were optimized at the B3LYP level of theory (shown in Figure S2). The C−C optimized values were then used for the C−C bond distances of the dicarboxylate linker in **6**, **8**, **12**, **13**, and **14**.

(25) Because the DFT calculations are sensitive to minor changes in the structural parameters, the high esd's (which are commonly observed) in the carbon−carbon bond lengths (~0.01 Å) of the polyolefinic linker render the results of the calculations susceptible to the sort of undulation seen in the blue trace in Figure 6.

(26) (a) Woodcock, H. L.; Schaefer, H. F., III; Schreiner, P. R. *J. Phys. Chem. A.* **2002**, *106*, 11923. (b) Plattner, D. A.; Houk, K. N. *J. Am. Chem. Soc.* **1995**, *117*, 4405.

(27) (a) Longuet-Higgins, H. C.; Salem, L. *Proc. R. Soc. London* **1959**, *A251*, 172. (b) Yannoni, C. S.; Clarke, T. C. *Phys. Rev. Lett.* **1983**, *51*, 1191. (c) Guo, H.; Paldus, J. *Int. J. Quantum Chem.* **1997**, *63*, 345.

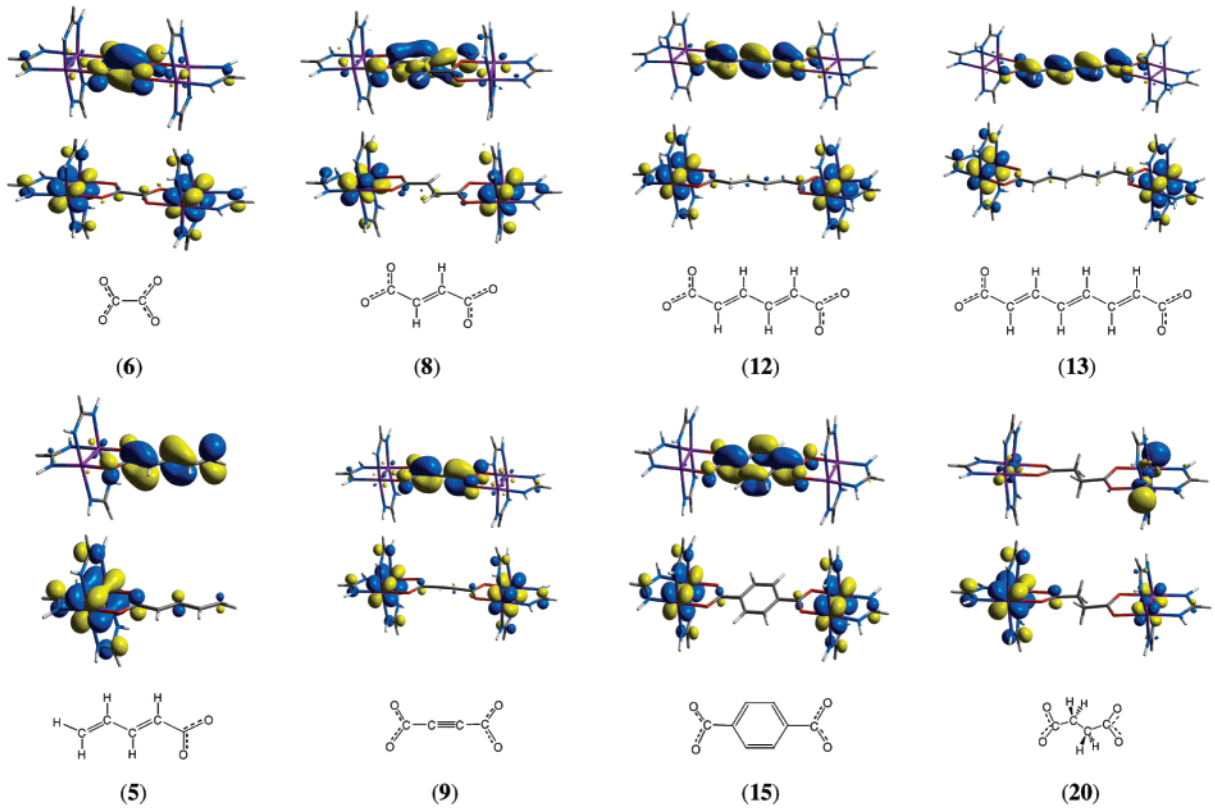

Figure 5. Illustrations of the 0.04 contour surface diagram of the DFT calculated HOMOs (upper in each pair) and LUMOs (lower in each pair) for compounds of the type $[Mo_2(DAniF)_3](O_2CXCO_2)[Mo_2DAniF)_3]$ and $[Mo_2(DAniF)_3](O_2CX)$ as identified by their carboxylate anions: oxalate, **6**; fumarate, **8**; *trans*,*trans*-muconate, **12**; tamuate, **13**; (*E*)-pentadienoate, **5**; acetylene dicarboxylate, **9**; terephthalate, **15**; succinate, **20**.

Table 1. Comparison of Calculated and Observed Lowest Energy Transitions

	calculated transition								
	using crystal structures			using partially optimized structures[24]			observed transition		
compd	eV	cm^{-1}	nm	eV	cm^{-1}	nm	eV	cm^{-1}	nm
3	3.09	24 900	401				2.79	22 500	445 (sh, 5000)
4	2.92	23 500	425				2.85	23 000	435 (sh, 4650)
5	2.41	19 500	514				2.73	22 000	454 (7750)
6	2.62	21 100	473	2.68	21 600	463	2.71	21 900	457 (9180)
7	2.33	18 800	532				2.39	19 300	519 (11 700)
8	2.20	17 700	564	2.27	18 300	546	2.33	18 800	533 (14 700)
9	2.41	19 500	514				2.66	21 400	467 (16 400)
10	2.82	22 700	440				2.85	23 000	435 (sh, 6690)
11	2.04	16 500	606				2.27	18 300	546 (13 400)
12	2.06	16 600	603	2.02	16 300	614	2.19	17 700	566 (16 100)
13	1.86	15 000	666	1.80	14 500	689	2.13	17 200	581 (18 100)
14	1.43	11 500	870	1.60	12 900	775	2.11	17 000	588 (19 300)
15	2.38	19 200	522				2.52	20 300	492 (15 200)
20	2.90	23 400	428				2.92	23 500	425 (sh, 4040)

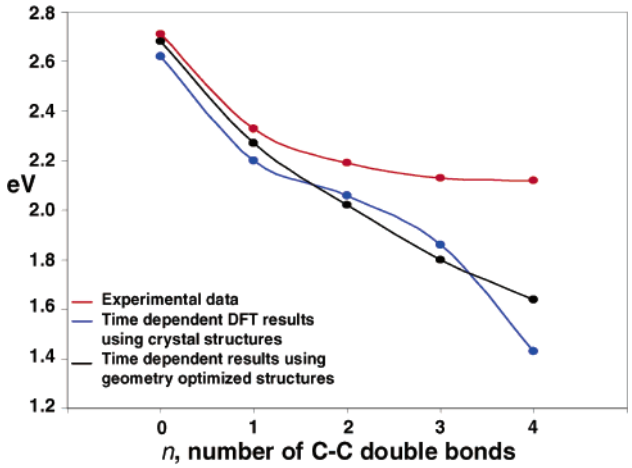

Figure 6. Plot of the calculated and observed HOMO to LUMO transition energies vs the number of carbon−carbon double bonds for the series $[Mo_2(DAniF)_3](O_2C(CH{=}CH)_nCO_2)[Mo_2DAniF)_3]$ ($n = 0-4$).

than the $\delta \rightarrow \pi^*$ charge transfer transitions. Those with chemically saturated linkers, such as **20** in Chart 1, have as their lowest energy absorption an essentially unperturbed $\delta \rightarrow \delta^*$ transition at higher energy rather than a metal-to-ligand charge transfer transition. The two Mo_2^{4+} units behave essentially as independent chromophores very similar to the homoleptic tetraformamidinate complexes $Mo_2(RNC(H)NR)_4$.[10]

Summary and Conclusions

Dicarboxylate linked pairs of Mo_2^{4+} display a strong dependence of the electronic ground and excited states upon the chemical nature of the linking species. With those linkers which are unsaturated and fully conjugated from end to end, the observed bands are best described as δ-to-π^*, metal-to-ligand charge transfer transitions. That these excitations are HOMO → LUMO transitions has been confirmed by time-dependent DFT calculations upon these molecules, where the expediency of substituting a hydrogen atom for the *p*-anisyl group has been employed. Those molecules with chemically saturated linkers, such as **20**, do not have mixing between the dicarboxylate ligand orbitals and the Mo_2 units and therefore have only relatively weak, relatively high energy localized $\delta \rightarrow \delta^*$ transitions as their lowest energy features. Our results are open to a very easily grasped explanation as to why the color of the fumarate linked

molecule, **8**, differs so significantly from that of the acetylene dicarboxylate linked molecule, **9**, despite having a lowest energy absorption of the same description. Since the carbon−carbon triple bond is appreciably shorter than the olefinic carbon−carbon bond, its π and π^* orbitals are proportionately lower and higher in energy, respectively, due to the increased orbital overlap. The $\delta \rightarrow \pi^*$ transition in **9** therefore occurs at a shorter wavelength (Figure 1) because the π^* orbital has been shifted upward in energy.

We find in our system of $[Mo_2(DAniF)_3](O_2C(CH{=}CH)_n\text{-}CO_2)[Mo_2(DAniF)_3]$ ($n = 0-4$) molecules a dependence of the lowest transition energy upon the length of the polyolefinic linker, which leads to a prediction as to where this feature should occur for the $n = 5$ and higher members. We note that dicarboxylates with alkynoic spacers have HOMO → LUMO metal-to-ligand transitions of the same type but with higher energy, and we anticipate that were the dicarboxylates $^{-}O_2C{-}(C{\equiv}C)_n{-}CO_2^{-}$ ($n = 2-4$) available, they would form a series of compounds with spectra qualitatively similar to those shown in Figure 2. These results also suggest that similar but even more pronounced effects will be observed with the molecular squares $[Mo_2(DAniF)_2]_4(O_2C(CH{=}CH)_nCO_2)_4$, in which each Mo_2 unit is directly linked to two others. Our results here differ qualitatively from the electronic spectra of other systems in which transition metal ions are joined by polyolefinic linkers. Each of the molecules in the series $(NH_3)_5Ru^{II}(py\text{-}(CH{=}CH)_npy)Ru^{II}(NH_3)_5$ $n = 2-4$ displays an intense band at ~545 nm, which has been attributed to a metal-to-ligand charge transfer transition. However, the energy and intensity of this band are essentially constant in this series,[28] possibly because of a disjunction between the pyridyl units and the polyolefinic fragment that keeps the charge transfer localized on the pyridyl groups.

(28) Woitellier, S.; Launey, J. P.; Spangler, C. W. *Inorg. Chem*. **1989**, *28*, 758.

The intimate electronic interactions between the Mo_2 units and the conjugated dicarboxylate linkers in compounds of the type $[Mo_2(DAniF)_3](O_2CXCO_2)[Mo_2(DAniF)_3]$ lead us to suggest that multiply bonded M_2 species of the sort extensively studied in this laboratory may serve as probes of the communication of electronic stimuli through conjugated systems. The use of M_2 units other than Mo_2^{4+} could provide a convenient means of shifting the MLCT into a particular energy range. In addition to its relevance to the preparation of molecule-scale electronic devices, the present work suggests how M_2 sensors could provide a new and different way of examining the excited state carotenoids that are proposed to form in the processes by which damaging free radical species are scavenged.

Acknowledgment. We thank the National Science Foundation and the Robert A. Welch Foundation for funding the research reported here. J.P.D. acknowledges the support of an NIH postdoctoral fellowship. We thank Dr. Kim Dunbar for access to the Shimadzu UV-1601PC spectrophotometer with which the absorption spectra were taken. We would like to thank the Laboratory for Molecular Simulation and Supercomputing facility at Texas A&M University for providing software and computer time. Helpful discussions with Dr. Michael B. Hall of Texas A&M University regarding the interpretation of the DFT calculations are gratefully acknowledged.

Supporting Information Available: Illustrations of the 0.04 contour surface diagram of the DFT calculated HOMOs and LUMOs for compounds **3**, **4**, **7**, **10**, **11**, and **14** are available as Supporting Information. Also available are the bond distances (Å) for the B3LYP optimized structures of the dicarboxylic acids used as analogues for the dicarboxylate linkers in **6**, **8**, **12**, **13**, and **14**. This material is available free of charge via the Internet at http://pubs.acs.org.

JA0343555